Design and feasibility of a pumping concept based on tritium direct recycling☆

T. Haertl [a],[*], C. Day [b], T. Giegerich [b], S. Hanke [b], V. Hauer [b], Y. Kathage [b], J. Lilburne [c], W. Morris [c], S. Tosti [d]

[a] EUROfusion Consortium, PPPT Department, Garching, Boltzmannstr. 2, Germany
[b] Karlsruhe Institute of Technology, Karlsruhe (KIT), Germany
[c] UKAEA-CCFE, Culham Science Centre, Abingdon, Oxfordshire, United Kingdom
[d] ENEA C.R., FSN Department, Frascati, Italy

ABSTRACT

In the DEMO Pre-Concept Design Phase, a novel fuel cycle architecture has been developed that aims at reducing the tritium inventory of the plant. In contrast to previous designs, the central role thereby is taken by an additional direct internal recycling loop. By already separating a significant proportion of the fuel at the pumping duct and providing this purified gas almost directly to the injection systems, the load on the tritium plant as well as the overall plant tritium inventory is reduced substantially. This paper summarizes the activities conducted in regard of integration and presents the results (aka the key design integration issues) for the design and feasibility of a pumping concept based on tritium direct recycling. The focus is on the aspects of integration of such a fuel separation function with the main technologies involved. In the functional position foreseen, these environment conditions mainly are space constraints, strong magnetic field, and the limited amount and restrictions in occupation of suitable ports. Two technical implementations for providing the fuel separation function have been identified: A metal foil pump relying on the physical phenomena of superpermeation of hydrogen through a metal membrane is able to provide continuous gas transfer. A multi-stage cryopump utilizing gas specific cryogenic trapping on several stages. Relying on gas binding, it only can operate intermittently. Within this activity, these variants are specifically reviewed for their suitability also to provide criteria for a future down selection.

1. Introduction

In the Pre-Conceptual Design (PCD) Phase activities for EU-DEMO (referred to as DEMO in this paper) [1], eight key design integration issues (KDIIs) [2] were identified as critical, either because the corresponding solution found in ITER is not suitable in DEMO or because the issues are DEMO-specific and not present in ITER.

The KDII7 activity summarised in this paper focusses on the integration issues of a pumping concept based on tritium direct recycling.

1.1. The EU-DEMO fuel cycle

Fundamental for the operation of a tokamak is the fuel cycle, the continuous process of providing the hydrogen fuel and noble gases - the

so called plasma enhancement gases (PEG) - to the plasma and removing the helium (He) ash and surplus gases from the region downstream of the divertor. In this paper "hydrogen" (Q_2) refers to all the isotopes, protium (H_2), deuterium (D_2), and tritium (T_2) and their isotopologues.

In the framework of the EUROfusion Programme within the technology work package tritium, matter injection and vacuum (WPTFV), a pre-conceptual design for the fuel cycle has been developed [3]. Driven by the requirements of a fusion power plant, a concept was developed that complies with the architecture and the pulsed way of operation of the DEMO tokamak. A novel three-loop architecture is intended to be applied for the fuel cycle [4]. It comprises the direct internal recycling loop (DIRL), the inner tritium plant loop (INTL) and the outer tritium plant loop (OUTL) as shown in Fig. 1.

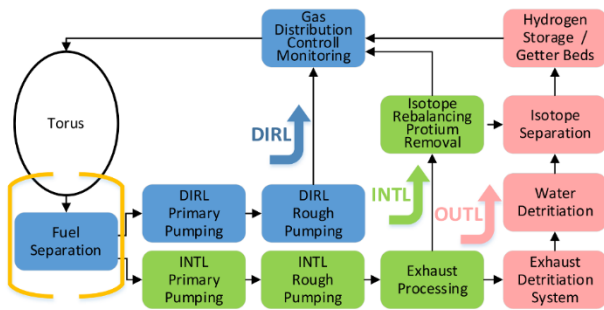The system block "fuel separation" plays a central role in it. Its

Fig. 1. Greatly simplified layout of the DEMO fuel cycle, omitting components for easier recognition and indicates the KDII7 area of study (orange brackets).

purpose is the separation of preferably highly pure hydrogen from the exhaust gas stream. Two possible technologies are presently identified and a pre-concept design for a technical implementation for each of these was developed. These are referred to here as the variants metal foil pump (MFP) and multi-stage cryogenic pump.

The exiting gas flows are individually compressed subsequently using a combination of specially designed diffusion (primary pumping) and liquid ring pumps (rough pumping) [5]. The hydrogen is routed directly to the gas distribution control and monitoring (GDCM) unit and made available for refuelling (DIRL). The remaining gas composition is prepared further in the exhaust processing (EP) system and the isotope rebalancing and protium removal (IRPR) system, where the majority of the residual hydrogen is separated and piped to the GDCM (INTL) supplemented by tritium from the breeding blanket. This then compensates the hydrogen being burnt to He or retained in the vessel and pipework. The low-in-hydrogen leftover gas mixture from the EP is further processed in exhaust detritiation (EDS) and water detritiation (WDS) systems. Finally, in the isotope separation system (ISS), residual tritium is separated and also piped to the GDCM via a buffer (OUTL).

A close link exists between the work conducted in this activity and WPTFV, which significantly contributed to this work. KDII7 focuses on integration aspects, mainly regarding the system block fuel separation (FS).

1.2. Critical considerations of the surrounding environment

The plasma operation in a fusion device relies on a high gas throughput. This is necessary to replace the small fraction of fuel burnt to He ash or trapped in materials, but mainly to provide the fuel density required to achieve high fusion power balanced against particle transport, and to provide hydrogen isotopes to dissipate power in the core, scrape-off and divertor plasma to protect the divertor target plates (via detachment). Additionally other gases are required to help keep the plasma detached and improve the radiation for the power exhaust. A
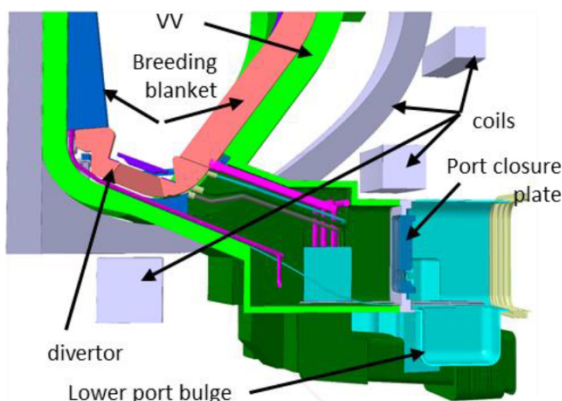
pumping system in a tokamak has to provide sufficient pumping speed to handle this throughput.

The pumping is best done in the divertor where neutral pressure is highest and the He and other impurities collect, noting that a high neutral pressure is needed for detachment. As well as for the single null (SN), but also for other considered configurations, e.g., a double null (DN) plasma configuration [6], it is beneficial to place the pumps close to the divertor, to maintain effective pumping performance and not create conductance losses arising from greater distance. This does not necessarily mean that the pumping equipment has to be located inside the vacuum vessel. Indeed, the typical set-up of vacuum systems is placing the pumps outside the main vacuum chamber.

Fig. 2 displays the bottom part of the vacuum vessel (VV) with the lower port in the 2019 design for a SN plasma configuration. Therein, the cross section of the VV and lower port (green), and the in-vessel components breeding blanket (blue, pink), divertor (pink) with liner (purple) are shown. Outside the VV, separated by the port closure plate (blue) is the port extension with the lower port bulge (turquoise) in the present design, and toroidal and poloidal field coils in the proximity of the lower port (grey).

Considering the intended position, several issues associated therewith are described in the following.

1.2.1. Divertor conductance

The divertor [7] extracts heat and provides neutron shielding of the VV and toroidal and poloidal field coils locally. Conflicting requirements exist between the shielding function by minimising opening, and the need to effectively pump requiring large opening. The particle exhaust of up to 450 $Pa.m^3.s^{-1}$ has to be ensured during plasma discharge at an indicative range of pressure between 1 - 10 Pa. The dwell phase has to be kept as short as possible and a final pressure of $\leq 1.5 \cdot 10^{-3}$ Pa has to be attained. The conductance is characterized by geometry, size, cross section, and number of gaps in the divertor. It has significant influence on the amount and the location of the downstream pumping performance required.

1.2.2. Space constraints

Size and shape of the lower port are mainly determined by the superconducting coil system and gravity support of the machine [8].

To alleviate the effects of reduced conductance, placing a pumping device close to the gas source (the divertor) is very beneficial for the primary pumping stage (providing the compression from molecular to viscous flow regime). This means that the integration of this pumping stage in the lower port would be best.

1.2.3. Number of pumping ports

The present DEMO baseline foresees 16 toroidal field coils as the best compromise between an adequate low ripple magnetic field and sufficient space in-between the coils for gravity supports and ports. Some of the 16 lower ports also have to be used for remote maintenance of the divertor and the impact of having pumps in the same ports is being investigated.

1.2.4. Magnetic field

The position close to the divertor, beneficial for pumping purposes, is in close vicinity to several magnetic field coils. Consequently, this means that the pumping components have to cope with a strong magnetic field. Not merely the range of the field strength (0.4 - 1.2 T), but also the heterogeneous and none-parallel nature (with varying inclinations) to the longitudinal axis of the installed pump are important. Additionally, transient electromagnetic fields are intrinsic with tokamak operation.

1.2.5. Neutron radiation

The impact of neutron radiation in the lower port is investigated elsewhere [9]. Calculations were carried out for different shielding concepts. The neutron flux and nuclear heating were calculated.

Fig. 2. Simplified illustration of the lower port with main components.

Although, these calculations are not intended to provide the functionality of the pumping equipment, they are useful to understand the problems, identify uncertainties and design improvements required. The main findings were:

- The neutron flux in the intended location of the pump is in the range of 10^{15} - 10^{16} neutron.m^{-2}.s^{-1} depending on shielding concept in the lower port.
- The port closure plate could provide a significant additional shielding effect, resulting in a reduction of the neutron flux behind by one order of magnitude.
- The nuclear heating loads at the intended location for the vacuum pump are around 10^3 W.m^{-3}.

1.2.6. Tritium environment

The fuel cycle has to cope with tritium in nearly all of the system blocks. The design generally considers this wherever it is necessary.

1.2.7. Remote maintenance

Due to the high radiation and the resulting activation, handling of components has to be executed remotely within the bioshield. This also includes the inspection, maintenance or replacement of all the pumping equipment. Investigations are necessary in regard of remote maintainability to find a suitable solution to handle the pumping equipment inside the port. As moving the pumping equipment is expected to be time consuming, ideally not all the lower ports should be used for pumping to allow the exclusive use of some of them for in-vessel activities. This leads to a significantly higher effort to move in-vessel components to the dedicated remote maintenance port. A trade-off has to be found to optimize time-efficiency. Comprehensive investigations are ongoing within work package remote maintenance (WPRM) including the pumping equipment. This task also considers failure scenarios [10]. Additionally, it must be considered that extensive repairs have to be carried out in the Active Maintenance Facility and components need to be transported there.

2. Variants of the fuel separation system block

To mitigate risks related to a premature single technology choice, two potential solutions for the system block fuel separation were developed. The two variants are the metal foil pump (MFP) and the multi-stage cryopump. In the following, the two technologies and related risks are briefly described.

2.1. Metal foil pump

2.1.1. Technology and design description

The effect of superpermeation [11] exclusively works for hydrogen (isotopologues). Thereby most of the energized hydrogen particles, sticking or implanted on a metallic surface permeate through. This fact is utilized in the MFP and a preliminary design has been elaborated. This foresees a thin-walled (0.1 mm) cylinder with a proposed diameter of 0.5 m and a length of 2 m made of the candidate material niobium (Nb)
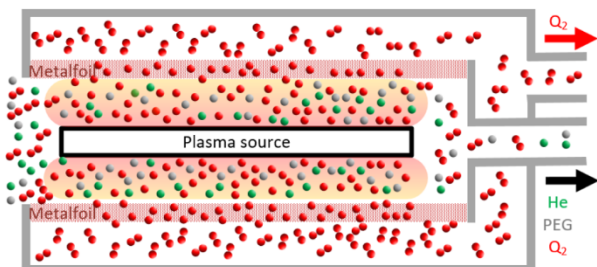
or vanadium (V). These values, whilst based on sound calculations considering several aspects, are still preliminary. Within the metal foil cylinder, a linearly extended plasma source, developed in cooperation with industry, is placed. This plasma source consists of an alumina tube containing a copper rod as inner conductor and providing an annular gap allowing for coolant agent gas flow. The plasma is generated by microwaves at a frequency of 2.45 GHz at the outer surface of the alumina tube [12]. This set-up allows generation of an extended homogeneous plasma up to several meters of length (see Fig. 3).

2.1.2. Risks associated with technology choice

Primary candidate materials for the metal foils need investigation for superpermeation function suitability, with the achievable throughput under various conditions and optimized operational temperature. The thin-walled foil material has to sustain the challenging occurring conditions also at stabilised elevated temperatures. When using resistance heating for temperature control, the metal foil cylinder might need a suitable support structure to withstand the resulting forces in a strong magnetic field. When realising the composite structure of foil material and support, some technological problems might occur. As a matter of fact, the coupling of different materials (V or Nb with the support) with different hydrogen uploading and thermal expansion / elongation could produce (high) mechanical stresses at the interfaces V/support (Nb/support). This can lead to the formation of defects/cracks (and loss of selectivity of the membrane). A key point for effective operation is the energizing of the particles in all given conditions. An influence of the strong magnetic field on the operability and shape of the plasma is to be expected. Ultimately, a design has to be developed to be integrated in the port's constructional dimensions.

2.2. Multi-stage cryopump

2.2.1. Technology and design description

For the reduction of pressure in vacuum applications, the trapping of gases on cryogenic surfaces is a common method and therefore generally it is a very mature technology. For the tasks of gas separation, a completely new arrangement of such a device is proposed.

In a standard setup for a cryopump, surfaces are operated at a suitable low temperature for condensation (or sorption) of the occurring mixture of gases. To achieve the separation functionality, it is foreseen to combine several surfaces in series, operated at different temperatures. Each of these surfaces provides the right temperature for trapping dedicated gas species at the given pressure conditions. A simplified schematic sketch of a multi-stage cryopump is shown in Fig. 4. The gas coming from the VV is entering from the left side, passing a baffle (red chevrons) operated at 80 K. At the first stage (yellow) operated at 20–30 K, the PEGs are condensed. At the second stage (green) all the hydrogen isotopologues are condensed at a temperature of 10–20 K. Finally, the He is sorbed at the last stage (blue), where the surfaces are coated with charcoal and cooled to 4.5 K. The choice of the optimum operation temperatures in such a three-stage configuration goes back to a detailed experimental study [13].
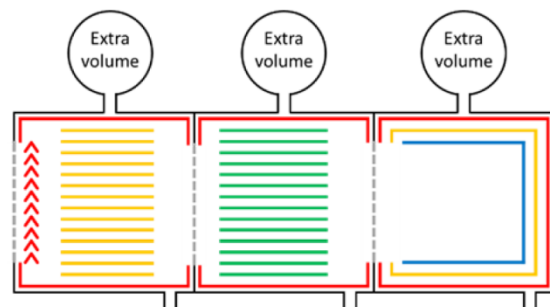

Fig. 3. Illustration of functional principle of MFP.

Fig. 4. Multi-stage cryopump concept with the different stages.

It has to be considered that gases are not transferred through, but trapped inside the pump (gas binding vacuum pumps). Consequently, a regeneration is required regularly (e.g. when the pumping speed is decreasing due to the build-up of ice layers, or for safety restrictions limiting the allowed inventory of burnable gases). Therefore, the panels are warmed up above the condensation temperature of the trapped gases and simultaneously the thawing gases are evacuated with the help of a suitable gas transfer pump. To prevent the defrosting gases from back streaming in the VV and to minimize mixing of the gases from different stages isolating valves at the entrance and in between the stages of the pump are necessary (see Fig. 11).

2.2.2. Risks associated with technology choice

During condensation and regeneration some mixing of the gas from the various cryo stages occurs. Thereby mainly the purity of the hydrogen fraction is of interest, as it influences the design of fuel cycle architecture.

The regeneration sequence requires the activation of the large-dimensioned gate valves, to be investigated for operability purposes. The space constraints in the lower port are challenging the design. The operation of cryopumps strongly depends on a reliable supply of coolant, for which gaseous (supercritical) He at different pressures for adapting to the various temperatures is foreseen. This contributes to the dimensioning of the entire cryo-plant and the accompanied energy consumption, which contributes to the DEMO power plant efficiency.

3. Discussion of results

3.1. Feasibility of the particle exhaust

The particle exhaust not merely depends on overall pumping speed but is mainly determined by the conductance of the divertor and the gas conditions right in front it. The feasibility of removing the expected amount of gas has been investigated comprehensively [14].

Input data is taken from the physical plasma code SOLPS [15], capable of providing neutral gas species densities in the scrape off layer close to the divertor. The SOLPS high resolution pressure profile (1000 values) was customized to 12 values along a "calculation line" (see Table 1). This limited number of values was taken as input for simulations with the ITERVAC code [16]. As a design support tool this code allows fast calculation of different variations. The real mechanical geometry is replaced by a network of channels representing shape, cross section, length and pressure at one estimated temperature. Fig. 5 shows a sketch of divertor (red), liner (purple), and the calculation line (black). The DEMO divertor has been modelled considering the pumping duct, divertor cassette, and cassette's pumping slot and gaps. The results show a high sensitivity of the calculated flows against the pressure distribution used as input.

The results of the ITERVAC simulations finally were benchmarked against results calculated with the DSMC method based DIVGAS (Divertor Gas Simulator) code [17]. DIVGAS considers real geometry, particle densities and temperature distribution and is thermodynamically consistent but has high computational needs.

The simulations results with ITERVAC towards DIVGAS show always higher pumped fluxes by a factor of 2 to 4 for deuterium and 6 to 7 for helium.

The ITERVAC results were scaled accordingly and should therefore now be realistic.

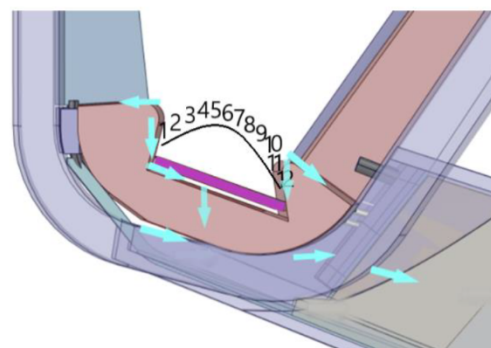The results for deuterium are shown in Fig. 6. The total pumped

Fig. 5. Illustrative diagram of the divertor (red), liner (purple), the values along the calculation line (black). For illustration purposes, some of the channels have been drawn in (turquoise arrows).

deuterium particle flux for using 16 (solid red) or 8 (dotted red) pumping ports is given for various effective pumping speeds in one of these ports. The flattening of the curves indicate that an increase in installed pumping speed does not contribute to an increase in throughput in the same way.
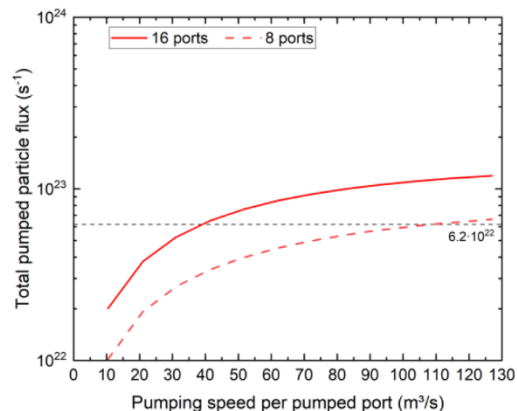

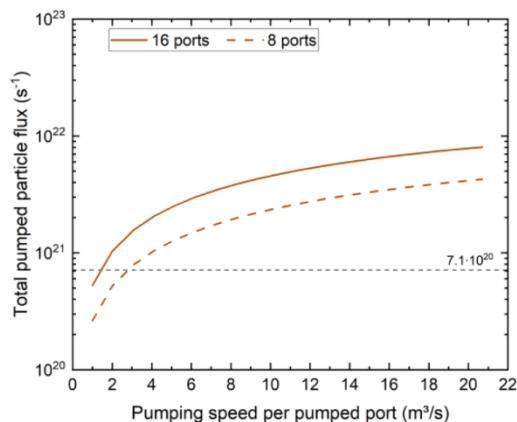**Fig. 6.** Pumped fluxes of deuterium depending on pumping speed per pumped port.

Fig. 7. Pumped fluxes of He depending on pumping speed per pumped port.

Table 1
2019 SOLPS values used for ITERVAC simulation.

#	1	2	3	4	5	6	7	8	9	10	11	12
P(D$_2$) [Pa]	2.12	1.91	1.02	0.76	0.67	0.69	0.62	0.63	0.61	0.57	0.57	0.64
P(He) [Pa]	0.60	1.07	0.32	0.18	0.13	0.10	0.09	0.08	0.09	0.10	0.13	0.25

This explains the high influence of the divertor and port conductance to the achievable overall pumping speed. The horizontal dotted black line thereby gives the minimum required flux in particles with the presently assumed fuel throughput of $\approx$230 Pa.m^3.s^{-1}. This clarifies that, even with highest pumping speed, using only 8 ports may not be sufficient to pump all the deuterium flux. Whereas a pumping speed of only $\approx$40 m^3.s^{-1} per port is sufficient, using all 16 ports.

In Fig. 7 the results for pumping the relatively small amount of He of $\approx$2.7 Pa.m^3.s^{-1} $\triangleq$ 7.1·10^{20} (s^{-1}) (dashed line) are shown. This is not seen as critical in case a pumping speed >4 m^3.s^{-1} per port is achieved.

A high degree of sensitivity on the pressure and its distribution in the divertor was recognized. For a divertor pressure below the assumed value of 1 – 10 Pa, the requirement on pumping speed is demanding. As SOLPS data have and will likely continue varying over time, all these calculations have to be regularly adapted to latest results.

3.2. Metal foil pump MFP

3.2.1. Test facility

For the research on material properties and energizing hydrogen for gaining a deeper insight on phenomenon of superpermeation, the test facility HERMES*plus* plays a central role [18]. The operation profited from additional resources provided from KDII activities.

The versatile facility (see Fig. 8) allowed for investigations in several areas. However as these are far beyond the scope of this document, only two major outcomes are included at this point, which are significant for integrational aspects.

Numerous experiment with the Nb foil operated at temperatures up to 1000 °C were performed. The influence on superpermeation of the upstream pressure (10 – 90 Pa) and the input power (1 – 3 kW) of the plasma source with a length of 0.3 m was thereby investigated.

The experiments showed that the permeation flux of hydrogen particles through the metal foil scales linearly with the applied microwave power to the plasma source.

In the range 15 – 60 Pa, the permeation flux only varies from 4 to 6 Pa.m^3.s^{-1}.m^{-2}. This is demonstrating that the permeation mechanism is not "pressure-driven" like for the common metal membranes (e.g. Pd-alloys) used in separation units for purifying hydrogen where the higher the pressure drop across the membrane the higher the permeation flux.

These results allow for an estimation of an achievable maximum throughput of up to 6 Pa.m^3.s^{-1}.m^{-2}. Deploying this result, a good estimation of the total required surface is possible. A full overview of recent experimental results, in particular on the plasma characterization and magnetic field influence, is given elsewhere [19].

3.2.2. Port integration

Parameters regarding the pumping are still to be decided, driven by uncertainties of an evolving design, by technical boundary conditions for manufacture and optimizing performance. In order to cope with this, an iterative workflow has been developed supporting the regular assessment of the required number of lower ports that have to be equipped with vacuum pumps. The conditions intertwined with the chosen plasma scenario - defined by physics (e.g. throughput, PEG quantity, and neutral gas pressure) - are used as input to decide engineering parameters on the pumping system (e.g. size, performance, number of pumps).

The following aspects are considered [20]:

- Useable space inside the lower port
- Suitable size of one MFP
- Integration of several MFPs to a common MFP-unit
- Assessment of resulting performance of the MFP-unit
- Calculation of required number of MFP-units for providing the required performance
- Estimation of the required pumping speed of the primary pumps backing the MFP-unit
- Integration of primary pumps
- Resulting number of lower port equipped with pumps

Using this methodology, a tentative design of the lower port with integrated MFP-unit accommodating 6 MFPs and a redesigned outer part of the port has been compiled (see Fig. 9). This arrangement now foresees the installation of the port closure plate (the barrier between high vacuum and atmosphere pressure) further inside the port. Outside the port closure plate additional space was created with the lower port bulge where the installation of some of the diffusion pumps is intended.

3.2.3. Number of ports and MFP-units

Applying the results available in [19], the following can be calculated: A total of 10 ports ($\pm$2) each equipped with MFP-units, housing 6 installed MFPs (diameter 0.5 m and length 2 m) are required for pumping the fuel. Presently, all components are in an early design state, which still involves high uncertainties of the performance.
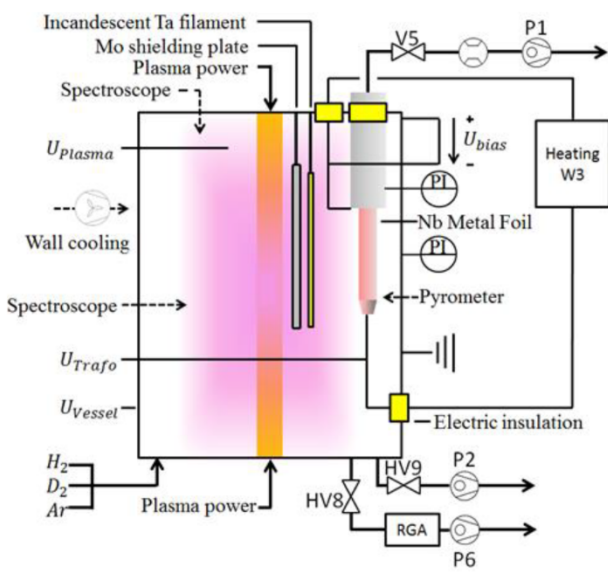

Fig. 8. Sketch of the HERMES*plus* test facility with additional installations during the experimental campaign of 2019.
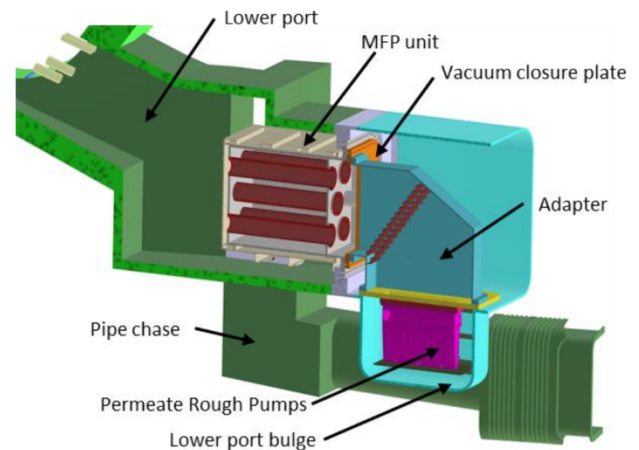

Fig. 9. Proposed setup of the MFP inside the lower port.

3.2.4. Magnetic field

In the position foreseen for the MFP the expected magnetic field strength is in the range 0.4 - 1.2 T [19]. Several possible impacts were identified and theoretically survey, as well as experimental investigation to proof the operability were undertaken:

Mechanical stability against magnetic forces. Additional heating is necessary to operate the metal foil at a stabilized temperature >700 °C. A common method is resistive heating, for which the foil material itself functions as an electrical conductor. Surrounded by a magnetic field, this results in strong mechanical forces of up to several hundred N (assuming: 2 m length, 0.1 mm thickness, several hundred A current, 1 T magnetic field perpendicular to the foil). The resulting shear stress on a foil without a support structure can be critical for denting and deformation. However, simulation of the mechanical stresses on such a foil with ANSYS confirmed that a foil of very basic geometry can withstand this, if given an adequate support structure.

Influence on suprathermal hydrogen production. The physical principle behind the superpermeation has been intensively investigated theoretically with literature studies. The findings have been reconfirmed with the use of the facility HERMES*plus*. All this gave proof that the fraction of atomic hydrogen exceeds by far any ionic hydrogen isotope and therefore, the superpermeation flux can be attributed mainly to atomic hydrogen. As this is neutral it is not affected by magnetic fields [19,21].

The production of dissociated hydrogen scales with the density of sufficiently energetic electrons for production of hydrogen atoms. Within the MFP, densities vary due to the electron's preferred trajectory along the field lines. Presently it is expected, that the total production rate for atomic hydrogen is independent of the presence of magnetic field, but density distribution is affected. Hence, no indication for impaired permeation performance for fuel separation in a magnetic field is given.

In cooperation with industry [12] the magnetic field test facility FLIPS (flexible linear plasma experiment) was used for experimental investigations (see Fig. 10) in a collaboration with the Institute of Interfacial Process Engineering and Plasma Technology at University of Stuttgart, Germany.

The facility allows for a plasma source parallel and perpendicular to the magnetic field lines and using protium and deuterium for the experiments. Due to technical realities, the magnetic field strength is limited to ≤250 mT, but this is already beyond the resonance condition (87 mT for 2.45 GHz). Therefore, extrapolation to higher fields is considered to be straightforward applying benchmarked plasma models. Conducted experiments showed plasma ignition and operation under most configurations, with sufficiently high plasma source power.
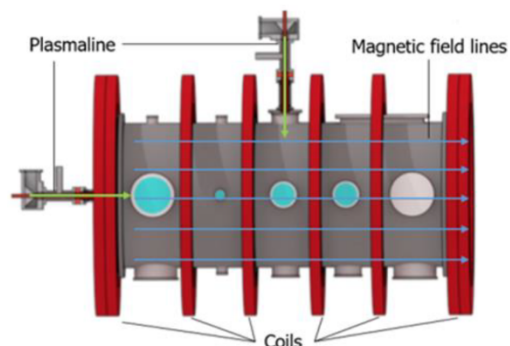

Fig. 10. Sketch of FLIPS facility with installed Plasmaline.

Further experiments also aim for inclined and transient magnetic fields.

3.2.5. Operation power

The power consumption of all DEMO plant auxiliary systems will contribute to the final DEMO electrical efficiency. Presently the power consumption of the fuel separation functionality of the pumping system could only be a rough estimation.

The set-up of the plasma source in the HERMES*plus* test facility has a length of ≈0.3 m, the input power for the tests done is presently ≈2 kW. The efficiency of magnetrons for microwave generation reaches ≈80%. Therefore an estimation for the power consumption of all the MFP pumps is as follows:

2 kW / 0.3 m (length of test source) x 2 m (MFP length) / 0.8 (efficiency) x 6 (MFPs/MFP-unit) x 10 (MFP-units) = 1.0 MW.

3.2.6. Remote maintenance

A short introduction to needs and activities of remote maintenance was given above.

The lower port configuration including the arrangement of the vacuum pumps has significantly changed within the time frame of the KDII activity, as part of a normal design progression, common in a PCD Phase. In the previous baseline design, the MFP-unit and primary pumps were foreseen to be mechanically combined as a line replacement unit and completely installed at the vacuum side of the lower port vacuum closure plate. The latest baseline design (see Fig. 9), has changed and only the MFP-unit is located inside the VV, whereas the primary pumps are outside. Therefore, some of the previous RM findings are not directly applicable to the latest baseline designs and therefore several concerns have to be addressed in future work. Various technical solutions have to be investigated or developed to comply with RM demands. Therefore in the Concept Design (CD) Phase, a close cooperation has to be foreseen between WPTFV and WPRM, ensuring the improving design of the pumping equipment is continuously verified for remote handling compatibility.

3.2.7. Tritium inventory

The MFP (in conjunction with primary- and rough pumps) form a continuously operating gas transfer vacuum pumping system. In steady state operation the inventory is hence mainly given by the amount of dissolved tritium in the metal foil material itself. The pre-concept calculation results foresee 10 ports equipped with MFPs of the actual design. The total metal foil surface is therefore ≈200 m^2 (thickness 0.1 mm). Operated at 700 °C, an amount of ≈10 g tritium can be estimated to be dissolved within the bulk of the candidate materials V or Nb. The amount of gaseous tritium (at given conditions e.g. pressure and temperature) can be expected with ≈1.5 g. The total tritium inventory in all the MFPs is therefore ≈11.5 g. This value is subject to significant further reduction (factor of 5) with the application of a more customized V-Pd alloy, possessing characteristics of reduced solubility and high mobility for the dissolved hydrogen.

3.3. Multi-stage cryopump

During the period of the KDII activities, the multi-stage cryopump has been improved to a pre-conceptual level. With an appropriate vacuum design (size, geometry and arrangement of the condensation and sorption surfaces) several simulations have been carried out.

3.3.1. Port integration

The aspects considered in the integration for the MFP (see section 3.2.2) are equally valid for the cryopump. The requirements on pumping are mainly independent on the technology used, and the position inside
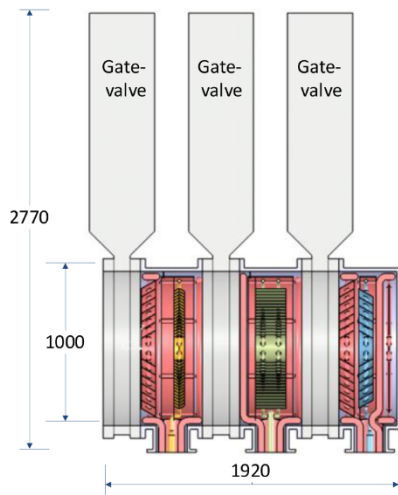
Fig. 11. Size indications of the multi-stage cryopump.

the lower port is expected to be comparable.

The inlet diameter of ≈1000 mm is defined by the required pumping speed. The indispensable gate valves are the size limiting components inside the narrowest part of the port (see Fig. 11). For space-integration aspects, the integration in the lower port is expected to be possible.

3.3.2. Number of ports and multi-stage cryopumps

As a principle of gas-binding vacuum pumps, periodic regeneration of the trapped gases is required as described in section 2.2. Compared to the foreseen 2 hour pulse duration of DEMO, the maximum pumping time for the cryopumps is significantly shorter, mainly due to limitation of the hydrogen inventory for reasons of explosion protection. Therefore, a staggered operation of the cryopumps is necessary, where at any point in time some of them are in pumping mode, whilst others are in regeneration mode or cooling down. This operating behaviour makes it necessary to have more installed pumps compared to gas transfer pumps of nominal similar pumping performance.

The performance of the multi-stage cryopump was simulated with DSMC (Direct Simulation Monte Carlo) code in the relevant pressure range (<1 - 10 Pa). The pumping speed is dependant on the inlet pressure and ranges from 33 $m^3.s^{-1}$ (@ 0.1 Pa) up to 110 $m^3.s^{-1}$ (@ 10 Pa). Therefore, throughput yields 75 $Pa.m^3.s^{-1}$ (@1 Pa) and >1000 $Pa.m^3.s^{-1}$ (@10 Pa). The values for the pumping speed for multi-stage cryopump and MFP are fairly comparable. Therewith, also at least 8 multi-stage cryopumps have to be simultaneously in pumping mode. The number of installed pumps is depending on the ratio between pumping time and the total time necessary for regeneration. This is estimated at 1/1 up to 1/3. A more complete description of the current multi-stage cryopump design is found elsewhere [22].

For the lowest expected inlet pressure (1 Pa) most of the lower ports have to be equipped with (at least) one multi-stage cryopump. At higher inlet pressures and/or with better pumping/regeneration rations this becomes less demanding. To cover all cases all lower ports should be equipped with a multi-stage cryopump.

3.3.3. Magnetic field

The influence of the DEMO magnetic field on the overall operation of the multi-stage cryopump wasn't investigated as a dedicated task. Generally, cryopumps are operated in comparable magnetic field strengths on different fusion devices (foreseen in ITER) without resulting in disclosed issues. Although the design of the multi-stage cryopump is unique, it is mainly the application of gate valves differing it to other cryopumps. Gate valves are also used in fusion devices under high magnetic fields without notable problems.

3.3.4. Operation power

An accurate calculation of the electrical power consumption for operating the multi-stage cryopump requires very detailed data of the design, material, weights, and mode of operation, which are presently not elaborated in this detail. Taking values from ITER, which is expected to have a comparable average gas throughput of 200 $Pa.m^3.s^{-1}$ (400 Pa. $m^3.s^{-1}$ peak), a rough estimation for DEMO is possible. Referred to in the specification for the ITER cryopumps including their local cold boxes, the average value of the equivalent cooling capacity at 4.5 K, is less than 15 kW. This would require up to 5 MW electrical power, based on the assumption it is taking 335 W_{el} for producing 1 W@4.0 K He.

3.3.5. Remote maintenance

The multi-stage cryopump was not included in the RM investigations yet, and no dedicated task has been performed for investigation within KDII7. Although completely different from the functional principle, the size, weight, number and type of connectors, is roughly comparable to that for the MFP. A significant difference may be the need for He at various temperatures down to ≈4 K, and the associated supply lines. These aspects are regularly affected for operation of other in-vessel components. Therefore, it is not expected that intractable circumstances arise from this, provided sufficient space is available. In principle, cryopumps have no wearing parts needing regular maintenance. This is different for the foreseen gate valves. The high frequency of operation likely determines the maintenance intervals. By applying catalogue data for a gate valve of the required size, scheduled inspection service should follow 10,000 open/close cycles. With the staggered operation an open/close cycle happens every 20 – 40 min. Therefore, maintenance for the multi-stage cryopump is necessary at least once a year.

3.3.6. Tritium inventory

Due to the gas-binding principle of operation, a cryopump builds up a gas inventory over the period of pumping. In a hydrogen dominated gas environment, the maximum pumping time is usually not constrained by saturation effects, but by safety related inventory limitations to avoid the risk of oxy-hydrogen explosion in any accident scenario. It hence depends on the number of pumps, the volume available for regeneration, and the cool-down times that have to be ensured by a sufficiently powerful cryo-supply. An economically feasible configuration for DEMO pumping yields in an accumulated tritium inventory (total value for all cryopumps installed) of 376 g (8 pumps) and 544 g (12 pumps), respectively.

The safety limit for the DEMO vacuum pump tritium inventory is preliminarily defined to 200 g. Therewith the estimated inventory of the multi-stage cryopump is about a factor of 2 higher. Compared to the inventory of the MFP, that one of the multi-stage cryopump is roughly 35 - 50 times higher.

3.3.7. Fuel separation performance

For the purpose of reducing the overall tritium inventory, the proposed DEMO fuel cycle relies on the separation of a high purity hydrogen fraction from all gas pumped out of the VV. Thereby, essentially two aspects are worthy of consideration and comparison to the corresponding performance data of the MFP. In this regard, vacuum flow simulations have been performed with the DS2V Direct Simulation Monte Carlo code [23].

The mean free path of particles becomes shorter with higher pressures. Therefore they are less efficiently pumped and more could pass the chevron's surfaces of the first condensation stages without colliding. As a consequence, the percentage of impurities (non-hydrogen gases) on the hydrogen stage increases with inlet pressure. The separation sharpness is defined as percentage of hydrogen trapped on the dedicated hydrogen stage in relation to the total amount of all gases on this stage. It indicates the purity of hydrogen available to be reinjected in the cycle without any further processing. In Fig. 12 left, it is shown that at the highest estimated
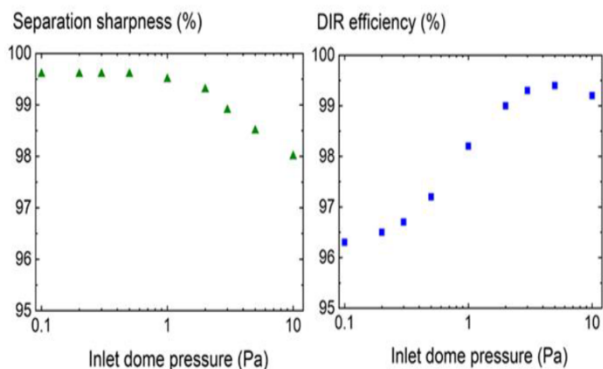
Fig. 12. Calculated hydrogen separation sharpness (left) and DIR efficiency (right) of the multi-stage cryopump.

inlet dome pressure the proportion of non-hydrogen gases is up to ≈2%.

The DIR efficiency is the percentage of the trapped hydrogen on the assigned stage relating the total pumped hydrogen on all the stages (almost exclusively the He stage). It is shown in Fig. 12 right, it is in excess of 98%.

Both results are very promising, but showing noticeable difference to the corresponding numbers of the MFP. A separation sharpness >98% (assumed value MFP: 100%), still implies a concentration of PEGs ≤2%, diluting the DT. The significantly larger value of the DIR efficiency (assumed value MFP: 80%) is not likely to provide additional benefit, as the size of the outer tritium plant loop cannot be reduced below a certain limit as it has to be designed for taking the tritium from the breeding blanket.

3.3.8. Fusion power and fuel purity

The concentration of PEGs in the core has influence on the attainable fusion power in the plasma. Simulations with the code ASTRA (Automated System for TRansport Analysis) [24–26] have been performed, evaluating the decrease in fusion power caused by fuel dilution and increased core radiation in presence of PEGs. The latter turned out to be the dominant contribution, especially in the case of the PEG argon. The calculation starts with an assumed concentration of PEGs in the pumped gas from divertor. The concentration of these PEGs in the fuel reinjected into the plasma is instead set by multiplying the divertor concentration times a variable factor (0 – 0.1).

The results of the calculations are shown in Fig. 13. If the PEG concentration in the reinjected fuel is reduced to 10% (0.1) of the
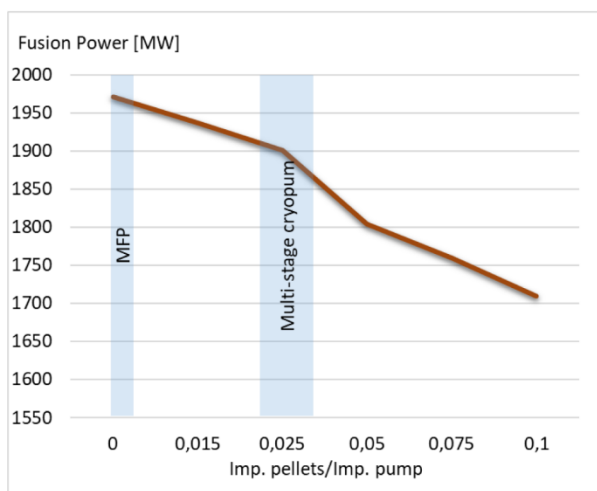

Fig. 13. Impact of the PEG concentration in reinjected fuel on fusion power (Courtesy of E. Fable).

concentration of the pumped gas, the resulting fusion power is reduced from 1971 to 1710 MW (by ≈13%). With the values for the separation sharpness of the multi-stage cryopump, a reduction of fusion power to 1901 MW (by ≈3.5%) could be expected.

The degradation of fusion power is mainly caused by the argon concentration. The concentration of xenon and He in the core are of much lower importance. The change of the mechanical properties of the pellets used for fuelling the plasma with an increasing content of PEGs was not part of this KDII investigation. Nevertheless, it is assumed that an increasing concentration has negative effects here as well.

4. Summary

The activities selected to further explore the identified integration issues have yielded valuable results. The design of DEMO VV and the lower port have noticeably advanced in the meantime but it is likely to be subject to further change. Pivotal for success in fulfilling the requirements from physics on the gas throughput for operating the plasma is the feasibility of the particle exhaust. Thereby, the design of the divertor and the number of lower ports equipped with pumps are decisive variables that cannot be compensated for by installation of larger pumping speed per port.

The MFP, as a prime candidate, has evolved considerably under investigation within WPTFV, and benefitted from supplementary resources. Most notably, an early adoption of investigations in light of the influence of the DEMO magnetic field on the MFP performance and mechanical stability was possible. The additional resources also made it possible to further characterise foil candidate materials in terms of a wide range of performance data. The formulation of a workflow for the integration of the MFP as well as the other involved pumps is substantial to adapt to further transforming conditions. All these investigations gave

Table 2
Fundamental characteristics for integration of MFP and multi-stage cryopump.

	MFP	Multi-stage cryopump
Operation mode	continuous	intermittent
Required number of pumping ports	Likely not all lower ports are necessary to provide sufficient pumping. Therefore 10^{+2}_{-2} are sufficient, leaving several available for RM without the need for removing pumps prior to divertor RM.	Based on the staggered mode of operation only part of the pumps are simultaneously in pumping mode. Therefore achieving the required pumping performance, considering also contingency, most likely all 16 lower ports be equipped with multi-stage cryopumps.
Lifetime / maintenance	MFPs have no wear parts to maintain, therefore no in-service inspection during ex-vessel maintenance shutdown is expected. If no solution for separating single MFPs is installed, failures call for in-vessel maintenance: Damage of metal foil (e.g. erosion) Contamination Pumping limitation through plasma source failures	For the special setup of the multi-stage cryopump involving several large gate valves, inspection of the gate valves at least once a year have to be considered, requiring removal of the pump.
Power consumption in operation	1.0 MW	Up to 5.0 MW
Tritium inventory	≈11.5 g	≈500 g
Procurement cost	Not assessed	Not assessed
Remaining impurities in the separated hydrogen stream	0%	Up to 2%
Fusion power using unprocessed gas for DIRL	1971 MW	1901 MW (reduction of ≈4%)

Table 3

Panel's recommendation for consideration in future activities.

#	Details of Recommendation
1	Since the final performance of the MFP is uncertain (immature technology), as are the divertor plasma requirements on neutral density, it is recommended that a holistic design is undertaken for the whole first stage pump system, i.e. MFP and upstream baffles etc., that aims to accommodate these uncertainties and allows for some degradation or even partial failures of the MFPs while meeting the DIR requirements of separation and the throughput limits of each MFP.
2	The design of MFP and multi-stage cryopump should examine in greater detail integration and maintainability aspects given their apparent complexity.
3	It is recommended further verification (especially testing) on effect of magnetic field and its gradients on MFP.
4	The future work plan should ensure a robust and timely development programme for the multi-stage cryopumps in case the MPF will not succeed.
5	The rather limited nature of the divertor plasma modelling so far leaves uncertainties in the pump performance and possibly reliability. It is recommended to take into account these design uncertainties that could impact the KDII7 and recommend link to KDII3 and KDII8.

reassurance that there are no serious issues expected evolving in the process of further maturation.

The multi-stage cryopump as a back-up solution has been developed to an early design stage and applied to substantial simulations. These comprised the pumping speed, separation sharpness, and DIR efficiency. Although numbers are promising and expected throughput is achievable, significant drawbacks are associated owing to the principles of operation. Staggered intermitted operation involves much higher tritium inventory and more ports have to be equipped with pumps.

Table 2 summarizes some of the fundamental findings. Both the MFP and multi-stage cryopump possess the ability to provide functional fuel separation. This encouraging result confirms the feasibility of the DIRL with the supplementary assurance of not relying on a single technology solution. However, only the MFP provides the hydrogen with the purity required and meets the preliminary tritium inventory target set by safety.

In the comprehensive process of developing the MFP to the present design state, no obstacle arose as of yet, but the overall maturity is still low. Therefore, it is vital to keep multi-stage cryopump as an alternative to reduce project risk, in a scenario where the MFP, as the most advantageous solution, does not evolve as expected.

From the time of initiation of the KDIIs it was planned to involve a panel for assessing the results of this work and finally approve these findings at gate review G1 [1] at the end of the PCD Phase. Two experts in the relevant field where nominated for taking this role. In Table 3 the recommendations provided by the panel are summarized which need to be considered in activities moving forward into the CD Phase.

CRediT authorship contribution statement

T. Haertl: Conceptualization, Methodology, Writing – original draft. **C. Day:** Conceptualization, Methodology, Writing – review & editing. **T. Giegerich:** Conceptualization, Methodology, Writing – review & editing. **S. Hanke:** Conceptualization, Methodology, Writing – review & editing. **V. Hauer:** Conceptualization, Methodology, Writing – review & editing, Software, Formal analysis. **Y. Kathage:** Conceptualization, Methodology, Writing – review & editing, Software, Formal analysis. **J. Lilburne:** Conceptualization, Methodology, Writing – review & editing. **W. Morris:** Writing – review & editing. **S. Tosti:** Writing – review & editing.

Declaration of Competing Interest

The authors declare that they have no known competing financial interests or personal relationships that could have appeared to influence the work reported in this paper.

References

[1] G. Federici, et al., The EU DEMO Staged Design Approach in the Pre-Concept Design Phase, this issue.

[2] C. Bachmann, et al., Key design integration issues addressed in the EU DEMO pre-concept design phase, Fus. Eng. Des. 156 (2020), 111595.

[3] Chr. Day, et al., The Pre-Conceptual Design of the DEMO Tritium, Matter Injection and Vacuum Systems, this issue.

[4] Chr. Day, et al., A smart three-loop fuel cycle architecture for DEMO, Fus. Eng. Des. 146 B (2019) 2462–2468.

[5] T. Giegerich, et al., Preliminary configuration of the torus vacuum pumping system installed in the DEMO lower port, Fus. Eng. Des. 146 B (2019) 2180–2183.

[6] H. Reimerdes, et al., Assessment of alternative divertor configurations as an exhaust solution for DEMO, Nuclear Fusion 60 (2020), 066030.

[7] G. Mazzone, et al., Eurofusion-DEMO divertor-cassette design and integration, Fus. Eng. Des 157 (2020), 111656.

[8] C. Gliss, et al., Initial integration concept of the DEMO lower horizontal port, Fus. Eng. Des 146 (2019) 2667–2670. B.

[9] D. Flammini, et al., Neutronics studies for the novel design of lower port in DEMO, Fus. Eng. Des. 146 (2019) 1394–1397.

[10] E. Organ, et al., Integration of service pipes into the lower port for the DEMO Double Null Concept Design Study, Fus. Eng. Des. 170 (2021), 112544.

[11] B.J. Peters, et al., Analysis of low pressure hydrogen separation from fusion exhaust gases by the means of superpermeability, Fus. Eng. Des. 124 (2017) 696–699.

[12] W. Petasch, et al., Duo-Plasmaline - a linearly extended homogeneous low pressure plasma source, Surface Coatings Technol. 93 (1997) 112–118.

[13] M. Scannapiego, et al., Experimental investigation on charcoal adsorption for cryogenic pump application, IOP Conf. Ser.: Mater. Sci. Eng. 278 (2017), 012160.

[14] F. Maviglia, et al., Impact of plasma-wall interaction and exhaust on the EU-DEMO design, Nucl. Mat. Energy 26 (2021), 100897.

[15] F. Subba, et al., SOLPS-ITER Modelling of Divertor Scenarios for EU-DEMO, Nucl. Fusion 61 (2021), 106013.

[16] V. Hauer, et al., Conductance modelling of ITER vacuum systems, Fus. Eng. Des. 84 (2009) 903–907.

[17] S. Varoutis, et al., Simulation of neutral gas flow in the JET sub-divertor, Fus. Eng. Des. 121 (2017) 13–21.

[18] S. Hanke, et al., Progress of the R&D programme to develop a metal foil pump for DEMO, Fus. Eng. Des. 161 (2020), 111890.

[19] Y. Kathage, et al., Experimental and simulation progress of a metal foil pump for fuel separation in the Direct Internal Recycling loop of DEMO, Fus. Eng. Des. submitted (2021).

[20] T. Giegerich, et al., Preliminary configuration of the torus vacuum pumping system installed in the DEMO lower port, Fus. Eng. Des. 146 B (2019) 2180–2183.

[21] A.I. Livshits, et al., Physico-chemical origin of superpermeability - Large-scale effects of surface chemistry on hot hydrogen permeation and absorption in metals, Journal of Nuclear Materials 170 (1990) 79–94.

[22] Chr. Day, et al., A multi-stage cryopump for fuel separation in the Direct Internal Recycling loop of DEMO, Fus. Eng. Des. submitted (2021).

[23] G.A. Bird, The DS2V/3V Program Suite for DSMC Calculations, in: Proceedings of the 24th International Symposium on Rarefied Gas Dynamics 762, AIP Conference Proceedings, 2005, pp. 541–546.

[24] G.V. Pereverzev, et al., ASTRA. An automatic system for transport analysis in a Tokamak, IPP Report (1991) 5–42.

[25] G.V. Pereverzev, et al., ASTRA automated system for transport analysis in a Tokamak, IPP Report (2002) 5–98.

[26] E. Fable, et al., Novel free-boundary equilibrium and transport solver with theory-based models and its validation against ASDEX Upgrade current ramp scenarios, Plasma Phys. Control. Fusion 55 (2013), 124028.